TAK1 is essential for endothelial barrier maintenance and repair after lung vascular injury

Dong-Mei Wang[†], Dheeraj Soni[†,‡], Sushil C. Regmi, Stephen M. Vogel, and Chinnaswamy Tiruppathi*
Department of Pharmacology and Regenerative Medicine, College of Medicine, University of Illinois, Chicago, IL 60612

ABSTRACT **TGF–β-activated kinase 1 (TAK1) plays crucial roles in innate and adaptive immune responses and is required for embryonic vascular development. However, TAK1's role in regulating vascular barrier integrity is not well defined. Here we show that endothelial TAK1 kinase function is required to maintain and repair the injured lung endothelial barrier. We observed that inhibition of TAK1 with 5Z-7-oxozeaenol markedly reduced expression of β-catenin (β-cat) and VE-cadherin at endothelial adherens junctions and augmented protease-activated receptor-1 (PAR-1)- or toll-like receptor-4 (TLR-4)-induced increases in lung vascular permeability. In inducible endothelial cell (EC)-restricted TAK1 knockout (*TAK1*$^{i\Delta EC}$) mice, we observed that the lung endothelial barrier was compromised and in addition, *TAK1*$^{i\Delta EC}$ mice exhibited heightened sensitivity to septic shock. Consistent with these findings, we observed dramatically reduced β-cat expression in lung ECs of *TAK1*$^{i\Delta EC}$ mice. Further, either inhibition or knockdown of TAK1 blocked PAR-1- or TLR-4-induced inactivation of glycogen synthase kinase 3β (GSK3β), which in turn increased phosphorylation, ubiquitylation, and degradation of β-cat in ECs to destabilize the endothelial barrier. Importantly, we showed that TAK1 inactivates GSK3β through AKT activation in ECs. Thus our findings in this study point to the potential of targeting the TAK1-AKT-GSK3β axis as a therapeutic approach to treat uncontrolled lung vascular leak during sepsis.**

Monitoring Editor
Jeffrey Hardin
University of Wisconsin, Madison

Received: Nov 9, 2021
Revised: Feb 24, 2022
Accepted: Mar 15, 2022

INTRODUCTION

TGF–β-activated kinase 1 (TAK1), also known as MAPKK kinase-7 (MAP3K7), is crucial in mediating inflammatory signals activated by cytokines and toll-like receptor ligands (Ninomiya-Tsuji *et al.*, 1999; Wang *et al.*, 2001; Adhikari *et al.*, 2007). TAK1 lies upstream of the NF-κB and MAPK signaling pathways (Adhikari *et al.*, 2007; Shim *et al.*, 2007). In B cells, TAK1 is required for B cell development and activation of NF-κB and MAPK signaling in response to TLR ligands and BCR stimuli (Liu *et al.*, 2006; Sato *et al.*, 2005; Schuman *et al.*, 2009), whereas TAK1 in neutrophils negatively regulates NF-κB and p38 MAP kinase activation (Ajibade *et al.*, 2012). A study using myeloid-specific TAK1 knockout mice showed that TAK1 restricts spontaneous NLRP3 inflammasome activation and cell death in macrophages (Malireddi *et al.*, 2018). TAK1 also suppresses RIPK1-dependent melanoma cell death (Podder *et al.*, 2019) and RIPK3-dependent endothelial necroptosis (Yang *et al.*, 2019). Global as well as endothelial cell (EC)-specific TAK1 deletion in mice resulted in embryonic lethality (Sato *et al.*, 2005; Morioka *et al.*, 2012). Inducible deletion of TAK1 in brain ECs suppressed interleukin 1β (IL-1β)-induced fever and lethargy (Ridder *et al.*, 2011). Deletion of TAK1 in ECs in a tamoxifen-inducible manner in adult mice showed that TAK1 was essential for the prevention of TNF–α-induced EC apoptosis (Naito *et al.*, 2019). However, it is unknown whether TAK1 signaling is essential for endothelial barrier maintenance and repair after lung vascular injury.

This article was published online ahead of print in MBoC in Press (http://www.molbiolcell.org/cgi/doi/10.1091/mbc.E21-11-0563) on March 24, 2022.

[†]These authors contributed equally.

[‡]Present address: Division of Infectious Diseases, Boston Children's Hospital, Harvard Medical School, Boston MA 02115.

*Address correspondence to: Chinnaswamy Tiruppathi (tiruc@uic.edu).

Abbreviations used: AJ, adherens junction; β-cat, β-catenin; BMDM, bone marrow-derived macrophage; CLP, cecal ligation and puncture; DAPI, 4′,6-diamidino-2-phenylindole; EBA, Evans blue dye–conjugated albumin; EC, endothelial cell; FBS, fetal bovine serum; GSK3β, glycogen synthase kinase 3β; HLMVEC, human lung microvascular endothelial cell; IB, immunoblot; IL-1β, interleukin 1β; mAb, monoclonal antibody; MAP3K7, MAPKK kinase-7; OZ, 5Z-7-oxozeaenol; pAb, polyclonal antibody; PAR-1, protease-activated receptor-1; Sc-siRNA, scrambled-siRNA; TAK1, TGF–β-activated kinase 1; TER, transendothelial monolayer resistance; TLR-4, toll-like receptor-4; TUNEL, terminal deoxynucleotidyl transferase dUTP nick end labeling; VE-cadherin, VE-cad; WT, wild type.

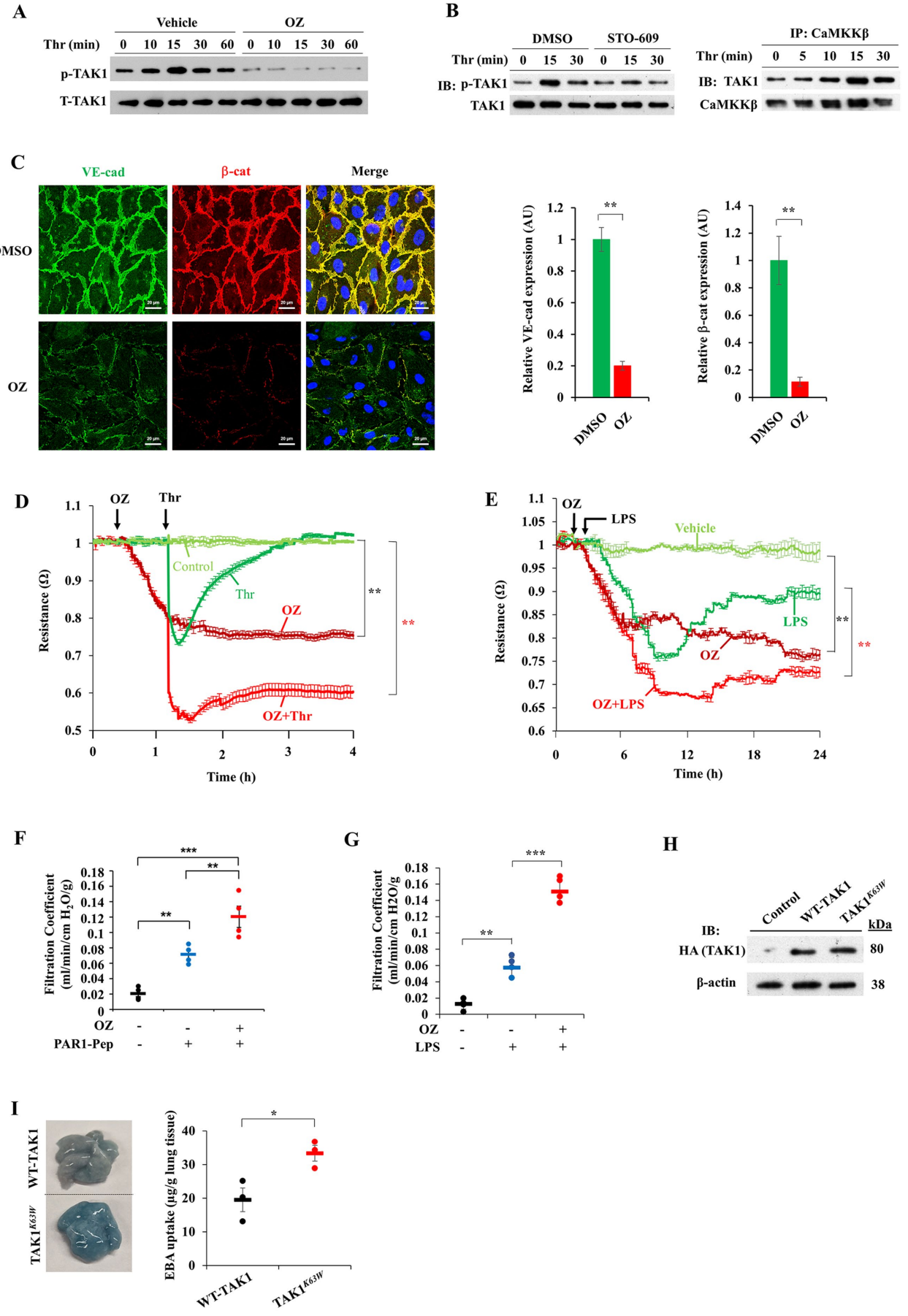
A
Vehicle
OZ
Thr (min) 0 10 15 30 60 0 10 15 30 60
p-TAK1
T-TAK1
B
DMSO
STO-609
Thr (min) 0 15 30 0 15 30
IB: p-TAK1
TAK1
IP: CaMKKβ
Thr (min) 0 5 10 15 30
IB: TAK1
CaMKKβ
C
VE-cad
β-cat
Merge
DMSO
OZ
Relative VE-cad expression (AU)
Relative β-cat expression (AU)
DMSO
OZ
D
OZ
Thr
Control
Thr
OZ
OZ+Thr
Resistance (Ω)
Time (h)
E
OZ
LPS
Vehicle
LPS
OZ
OZ+LPS
Resistance (Ω)
Time (h)
F
Filtration Coefficient (ml/min/cm H2O/g)
OZ
PAR1-Pep
G
Filtration Coefficient (ml/min/cm H2O/g
OZ
LPS
H
Control
WT-TAK1
TAK1K63W
IB:
kDa
HA (TAK1)
80
β-actin
38
I
WT-TAK1
TAK1K63W
EBA uptake (μg/g lung tissue)
WT-TAK1
TAK1K63W

Endothelial barrier dysfunction results in protein-rich edema formation and inflammatory cell infiltration that characterize diseases, for example, acute respiratory distress syndrome (Goldenberg *et al.*, 2011; Matthay and Zemans, 2011). In the inflammatory context, endothelial barrier integrity is highly dependent on the processes governing endothelial barrier repair. VE-cadherin (VE-cad) forms Ca^{2+}-dependent homophilic *cis* and *trans* dimers at adherens junctions (AJs) that establish cell-to-cell adhesion, essential for endothelial barrier integrity (Dejana *et al.*, 2008; Komarova and Malik, 2010; Goddard and Iruela-Arispe, 2013). The association between β-catenin (β-cat) and VE-cad is essential for the formation of endothelial AJs (Dejana *et al.*, 2008; Komarova and Malik, 2010). In septic patients and animal models of sepsis, the lung is the first organ to fail due to loss of endothelial barrier function (Goldenberg *et al.*, 2011). Phosphorylation of the AJ protein VE-cad and its associated protein, β-cat, promotes loss of endothelial barrier integrity (Nottebaum *et al.*, 2008; Chen *et al.*, 2012; Orsenigo *et al.*, 2012; Gong *et al.*, 2014; Wessel *et al.*, 2014; Soni *et al.*, 2017). Since ablation of TAK1 expression in ECs resulted in embryonic lethality in mice, we investigated whether TAK1 signaling, by controlling expression of AJ components, is essential for maintenance of endothelial barrier integrity. Our results for the first time show that endothelial TAK1 kinase function is required to maintain and repair the injured lung endothelial barrier. Mechanistically, we demonstrate that TAK1 maintains and repairs the endothelial barrier after lung injury through AKT-dependent inactivation of glycogen synthase kinase 3β (GSK3β), which in turn increases β-cat expression at AJs to stabilize the endothelial barrier.

RESULTS

Inhibition of TAK1 activity disrupts the endothelial barrier

Autophosphorylation of TAK1 at Thr-187 in the activation loop promotes the catalytic activity of TAK1 (Singhirunnusorn *et al.*, 2005). In our initial experiments, 5Z-7-oxozeaenol (OZ), a widely recognized TAK1-specific inhibitor, was used to block TAK1 kinase activity (Fechtner *et al.*, 2017; Malireddi *et al.*, 2018; Naito *et al.*, 2019). First, we determined the effect of OZ on TAK1 activation in ECs. We observed that OZ blocked thrombin-induced phosphorylation of Thr-187 in the TAK1 activation loop (Figure 1A). Since Ca^{2+}-dependent protein kinases are known to activate TAK1 (Ishitani *et al.*, 2003), we studied whether CaMKKβ, activated downstream of PAR–1-induced Ca^{2+} influx (Sundivakkam *et al.*, 2013), is involved in TAK1 activation in ECs. We observed that the CaMKKβ-selective inhibitor STO-609 blocked thrombin-induced autophosphorylation of TAK1 in ECs (Figure 1B). We also followed the interaction between TAK1 and CaMKKβ in response to thrombin (Figure 1B) with the aid of immunoprecipitation, which indicated that CaMKKβ activation downstream of protease-activated receptor-1 (PAR-1) mediates TAK1 phosphorylation. Next, we determined the effect of OZ on endothelial barrier integrity by measuring the expression of VE-cad and β-cat at EC AJs. Interestingly, we observed that OZ treatment markedly reduced expression of VE-cad and β-cat at EC AJs (Figure 1C). Measurement of transendothelial monolayer resistance (TER) showed that OZ itself caused a time-dependent decrease in TER (Figure 1D), indicative of disassembly of endothelial AJs. Further, we observed that the PAR-1 agonist thrombin (generated in the vasculature during sepsis) produced a transient increase in permeability, whereas LPS produced a sustained increase in permeability as reflected by the relative decrease in TER (Figure 1, D and E); however, both responses were more sustained and pronounced with OZ treatment as compared with controls (Figure 1, D and E). Next, to address the effect of TAK1 kinase inhibition on intact lung vascular barrier integrity, we measured PAR–1-activating peptide (TFLLRNPNDK)-induced changes in the pulmonary transvascular fluid filtration coefficient ($K_{f,c}$), a measure of endothelial liquid permeability in mouse lungs, and observed a threefold increase in $K_{f,c}$ over the basal value in wild-type (WT) mouse lungs (Figure 1F), whereas in mouse lungs perfused with OZ for 30 min, the PAR–1-induced increase in $K_{f,c}$ (Figure 1F) was significantly augmented. Perfusion with OZ alone for 30 min had no significant effect on basal permeability (data not shown). WT mice, challenged with a low dose of LPS (5 mg/kg, i.p.) for 6 h and then exposed to OZ as above, showed a similar augmentation of endothelial permeability increase (Figure 1G). Next, we used a liposome-mediated gene delivery method in lung ECs in vivo (Zhou *et al.*, 1998; Tiruppathi *et al.*, 2014; Soni *et al.*, 2018) to address whether TAK1 kinase function is required for endothelial barrier integrity. We observed that forced expression of a kinase defective TAK1 ($TAK1^{K63W}$) mutant in mouse

FIGURE 1: Inhibition of TAK1 kinase activity causes loss of endothelial barrier function. (A) HLMVECs treated with 1 μM OZ or vehicle (control) for 1 h at 37°C were exposed to thrombin (25 nM) for different time intervals. Then, cell lysates were subjected to IB analysis to assess phosphorylation of Thr-184/187 ($p^{T184/187}$) in the TAK1 activation loop. (B) HLMVECs were treated with CaMKKβ inhibitor STO-609 (1 μM) or vehicle (DMSO) for 30 min and then thrombin-induced phosphorylation of TAK1 was measured (*left* panel). *Right* panel, after thrombin treatment, cell lysates were immunoprecipitated and blotted with indicated antibodies. Results shown in A and B are representative of two separate experiments. (C) HLMVECs grown on coverslips were treated with 1 μM OZ or vehicle (control) for 1 h at 37°C. After treatment, cells were stained with antibodies specific to VE-cad (green), β-cat (red), and DAPI (blue) and analyzed by confocal microscopy. Experiment was repeated 3×. The bar graph summarizes the quantitative analysis of VE-cad and β-cat expression at cell–cell junctions. Results shown are mean ± SE relative fluorescent intensity compared with untreated cells. AU, arbitrary units; $n = 5$–8 cells per group; $^{**}p < 0.001$. (D, E) HLMVECs grown to confluence were used to measure real-time changes in TER to assess endothelial barrier integrity. Arrows indicate time of OZ (1 μM), vehicle (DMSO), thrombin (25 nM) (D), or LPS (1 μg/ml) addition (E). Values from three experiments are plotted as mean ± SEM. $^{**}p < 0.001$ compared with control. (F) PAR-1 agonist peptide-induced increase in pulmonary transvascular liquid filtration coefficient ($K_{f,c}$) in WT mice was measured in the presence and absence of TAK1 inhibitor OZ. Lungs were perfused for 30 min with OZ (1 μM) or vehicle (DMSO) and then PAR-1 agonist peptide was used to induce an increase in $K_{f,c}$. $N = 5$ mice per group. $^{**}p < 0.001$; $^{***}p < 0.0001$. (G) WT mice were challenged with LPS (5 mg/kg, i.p.) or saline for 6 h and then lungs were harvested for $K_{f,c}$ measurement as above with or without OZ (1 μM) pretreatment. $N = 5$ mice per group. $^{*}p < 0.01$; $^{**}p < 0.001$. (H, I) WT mice were injected i.v. with liposome-TAK1 plasmid construct (HA-WT-TAK1 or HA-$TAK1^{K63W}$) complex. (H) At 72 h after injection, lungs harvested were used for IB analysis. (I) At 72 h after injection, mice were used to assess in vivo lung vascular permeability by measuring EBA uptake in lung tissue. $N = 4$ mice per group. $^{*}p < 0.01$.

lung ECs significantly increased basal lung vascular permeability, as assessed by Evans blue dye–conjugated albumin (EBA) uptake in lung tissue compared with WT-TAK1 (Figure 1, H and I). These findings together show that TAK1 kinase function is essential for maintenance of endothelial barrier integrity.

Endothelial deletion of TAK1 disrupts the endothelial barrier and induces inflammation

To study the in vivo role of endothelial TAK1, we created tamoxifen-inducible EC-restricted TAK1 knockout (*TAK1*$^{i\Delta EC}$) mice and confirmed that TAK1 was not expressed in ECs of *TAK1*$^{i\Delta EC}$ mice (Figure 2, A–C). Hematoxylin and eosin staining of lung sections from *TAK1*$^{i\Delta EC}$ mice showed perivascular infiltration of inflammatory cells and hemorrhage as compared with tamoxifen-treated *TAK1*$^{fl/fl}$ (WT) mice (Figure 2D). To determine whether EC-expressed TAK1 affects vascular barrier integrity, we first measured the pulmonary transvascular fluid filtration coefficient ($K_{f,c}$) using isolated murine lung preparations. Interestingly, we observed an eightfold increase in the basal $K_{f,c}$ value in *TAK1*$^{i\Delta EC}$ lungs compared with WT (Figure 2E). Next, we assessed EBA uptake in lung tissue with or without LPS challenge. Here we observed that basal as well as LPS-induced EBA uptake were augmented in *TAK1*$^{i\Delta EC}$ mice compared with *TAK1*$^{fl/fl}$ mice (Figure 2F). *TAK1*$^{i\Delta EC}$ mice challenged with a low dose of LPS (5 mg/kg, i.p.) exhibited 100% mortality within 24 h (Figure 2G), whereas all WT mice survived for the 6-d observation period (Figure 2G). We also observed that *TAK1*$^{i\Delta EC}$ mice were highly susceptible to polymicrobial sepsis induced by cecal ligation and puncture (CLP) compared with their WT counterparts (Figure 2H). To address whether the endothelial barrier disruption in *TAK1*$^{i\Delta EC}$ mice is the result of endothelial apoptosis, we performed terminal deoxynucleotidyl transferase dUTP nick end labeling (TUNEL) staining. We did not observe TUNEL-positive ECs in lungs of either *TAK1*$^{i\Delta EC}$ or *TAK1*$^{fl/fl}$ mice (Figure 3A). Knockdown of TAK1 in human lung microvascular ECs (HLMVECs) also did not induce apoptosis (Figure 3B), indicating that TAK1 deficiency did not induce barrier breakdown due to apoptosis of ECs.

Endothelial TAK1 signaling is required to restore the endothelial barrier after toll-like receptor-4 (TLR-4)-induced vascular barrier breakdown

Since the *TAK1*$^{i\Delta EC}$ mice showed increased basal lung vascular permeability (Figure 2, E and F) and increased mortality after LPS or CLP challenge (Figure 2, G and H), we determined TAK1 expression in ECs after LPS challenge. We observed that LPS challenge caused a time-dependent decrease in TAK1 expression in ECs, which was restored to baseline levels within 24 h of LPS treatment (Figure 4A). Next, we determined the effect of LPS on TAK1 expression in mouse lungs in vivo. We showed above that LPS (5 mg/kg, i.p.) challenge caused lung vascular leak at 6 h in WT mice (Figure 2F); however, in survival experiments, LPS at a dose of 5 mg/kg failed to induce mortality in WT mice (Figure 2G), suggesting that this low dose of LPS (5 mg/kg) is not sufficient to sustain the lung injury response in WT mice. Thus we injected WT mice with a higher dose of LPS (10 mg/kg, i.p.) for different periods of time to assess the LPS effect on TAK1 expression in lung tissue. Here we observed that LPS challenge caused an initial loss of TAK1 expression in lungs of WT mice, which returned to baseline levels within 24 h of LPS challenge (Figure 4B). In WT mice, the time course of LPS-induced down-regulation and re-expression of AJ proteins β-cat and VE-cad was positively correlated with TAK1 expression (Figure 4C). We did not observe re-expression of β-cat and VE-cad in lungs of *TAK1*$^{i\Delta EC}$ mice after LPS (10 mg/kg, i.p.) challenge, because these mice failed to survive for more than 6 h after LPS challenge (Figure 4C). These findings collectively support the concept that the EC TAK1 expression induced during vascular injury may be required to repair the injured endothelial barrier.

TAK1 inhibition of GSK3β prevents β-cat degradation and maintains endothelial barrier function

VE-cad–β-cat interaction at endothelial AJs maintains endothelial barrier integrity (Dejana *et al.*, 2008; Komarova and Malik, 2010). To examine the mechanisms of TAK1-induced endothelial barrier protection, we focused on the expression of AJ protein β-cat in TAK1-deficient ECs. Here we treated ECs from *TAK1*$^{fl/fl.Cre+}$ mice with tamoxifen (2 μM) for 72 h to conditionally delete TAK1 (Figure 5A), which in turn reduced β-cat expression by ~80% as compared with control ECs (Figure 5A). We also observed markedly reduced expression of β-cat and VE-cad in lungs of *TAK1*$^{i\Delta EC}$ mice compared with *TAK1*$^{fl/fl}$ mice (Figure 5B). β-cat contains several consensus phosphorylation sites (S29, S33, S37, T41, S45) for GSK3β (Aberle *et al.*, 1997). GSK3β phosphorylation of β-cat promotes β-cat ubiquitylation and degradation via the proteasomal pathway (Aberle *et al.*, 1997; Wang *et al.*, 2014), and inhibition of GSK3β has been linked to enhanced endothelial barrier function due to increased β-cat expression at AJs (Ramirez *et al.*, 2013). Thus we addressed the possibility that TAK1 inhibits GSK3β and thereby stabilizes β-cat at AJs to promote barrier function. We observed that TAK1 inhibitor OZ prevented basal as well as thrombin- or LPS-induced phosphorylation of GSK3β at S9 (Figure 5, C and D), which blocks the catalytic function of GSK3β (Cohen and Frame, 2001). Knockdown of TAK1 also suppressed phosphorylation of GSK3β at S9 in ECs (Figure 5E), suggesting that TAK1 inhibition leads to increased phosphorylation of β-cat, increased β-cat degradation, and hence decreased β-cat expression at AJs. To address whether this is the case, we determined phosphorylation of the S33, S37, and T41 β-cat residues and observed that thrombin- and LPS-induced phosphorylation of β-cat was increased in OZ-treated ECs (Figure 6, A and B). Next, to address whether the proteasomal pathway was responsible for β-cat degradation, we determined the effects of TAK1 inhibition on β-cat ubiquitylation. We observed that basal as well as thrombin- and LPS-induced ubiquitylation of β-cat was increased in OZ-treated ECs (Figure 6, C and D). Since OZ treatment disrupted the endothelial barrier (Figure 1, C–G), we determined the effect of GSK3β inhibition on OZ-induced endothelial barrier disruption. Pretreatment with the GSK3β inhibitor largely prevented OZ-induced loss of VE-cad and β-cat at AJs (Figure 6E) as well as OZ- plus thrombin- or LPS-induced decreases in TER (Figure 6, F and G). These results show that TAK1-mediated inhibition of GSK3β prevents β-cat degradation and hence promotes β-cat localization at AJs to maintain endothelial barrier integrity.

TAK1 activates AKT to suppress the function of GSK3β in ECs

Since we observed that inhibition of TAK1 blocked phosphorylation of GSK3β at S9, we addressed the possibility that TAK1 inactivates GSK3β through AKT activation, which is known to phosphorylate GSK3β at S9 and thereby inactivate the kinase (Wang *et al.*, 2014; Cohen and Frame, 2001). OZ treatment blocked thrombin- and LPS-induced phosphorylation of AKT (Figure 7, A and B). Moreover, either thrombin or LPS stimulation caused interaction between TAK1 and AKT in ECs (Figure 7C). In addition, an AKT inhibitor prevented thrombin- or LPS-induced S9 phosphorylation of GSK3β

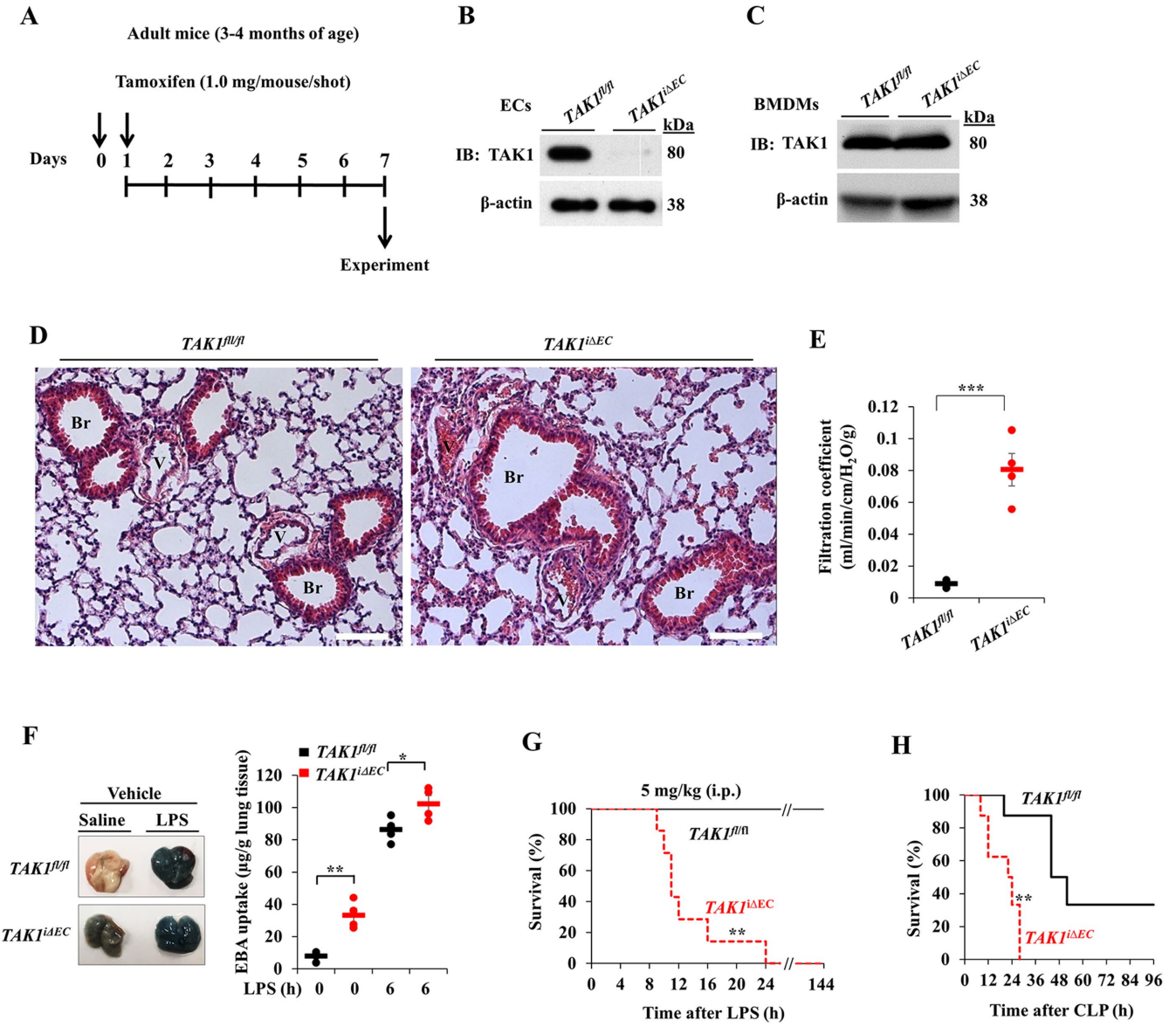

FIGURE 2: EC-restricted TAK1 deletion in mice causes basal lung vascular leak and increases susceptibility to sepsis. (A-C) *EC-restricted tamoxifen-inducible TAK1 deletion in mice.* (A) Timeline of tamoxifen administration. *TAK1*$^{fl/fl}$ and TAK1$^{fl/fl/Scl\text{-}CreERT2+}$ mice received an i.p. injection of tamoxifen to delete TAK1 in TAK1$^{fl/fl/Scl\text{-}CreERT2+}$ mice (*TAK1*$^{i\Delta EC}$). (B) Lung endothelial cells (LECs) from *TAK1*$^{fl/fl}$ and *TAK1*$^{i\Delta EC}$ mice were subjected to IB to determine TAK1 expression. (C) BMDMs from *TAK1*$^{fl/fl}$ and *TAK1*$^{i\Delta EC}$ mice were subjected to IB to determine TAK1 expression. (D–H) *TAK1 deficiency in ECs induces lung vascular leak and augments sepsis-induced lung injury.* (D) Hematoxylin and eosin staining of lung sections from *TAK1*$^{fl/fl}$ and *TAK1*$^{i\Delta EC}$ mice. Scale bars, 100 μm; Br, bronchi; V, vessel. (E) Pulmonary transvascular liquid filtration coefficient in lungs of *TAK1*$^{fl/fl}$ and *TAK1*$^{i\Delta EC}$ mice. $N = 5$ mice per genotype. $^{**}p < 0.001$, *TAK1*$^{fl/fl}$ vs. *TAK1*$^{i\Delta EC}$. (F) *TAK1*$^{fl/fl}$ and *TAK1*$^{i\Delta EC}$ mice injected i.p. with either saline or LPS (5 mg/kg) for 6 h and used to assess lung vascular leak by measuring EBA uptake. Representative lung images are shown in the left panel. Quantified results are shown in the right panel. $N = 5$ mice/genotype. $^{**}p < 0.001$. (G) Survival of age- and sex-matched *TAK1*$^{fl/fl}$ and *TAK1*$^{i\Delta EC}$ mice after administration of LPS (5 mg/kg, i.p.). $N = 10$ mice per genotype; $^{**}p < 0.001$ compared with *TAK1*$^{fl/fl}$ (log-rank test). (H) Survival of age- and sex-matched *TAK1*$^{fl/fl}$ and *TAK1*$^{i\Delta EC}$ mice after CLP. $N = 10$ mice per genotype; $^{**}p < 0.001$ compared with *TAK1*$^{fl/fl}$ (log-rank test).

(Figure 7, D and E). Furthermore, AKT inhibition augmented basal as well as thrombin- or LPS-induced permeability increase as assessed by TER (Figure 7, F and G). Taken together, these results suggest that TAK1 activates AKT which in turn inactivates GSK3β to restore the endothelial barrier. Based on these findings, we propose a model (Figure 7H) in which TAK1 inhibits the function of GSK3β via AKT to regulate the endothelial barrier.

DISCUSSION

Loss of vascular barrier integrity due to the breakdown of endothelial AJs is a hallmark of acute vascular injury (Matthay *et al.*, 2019; Goldenberg *et al.*, 2011). A key pathogenic mechanism underlying the breakdown of AJs is the down-regulation of cell–cell interacting VE-cad and its associated protein β-cat (Goldenberg *et al.*, 2011; Carmeliet *et al.*, 1999; Cattelino *et al.*, 2003; Mirza *et al.*, 2010).

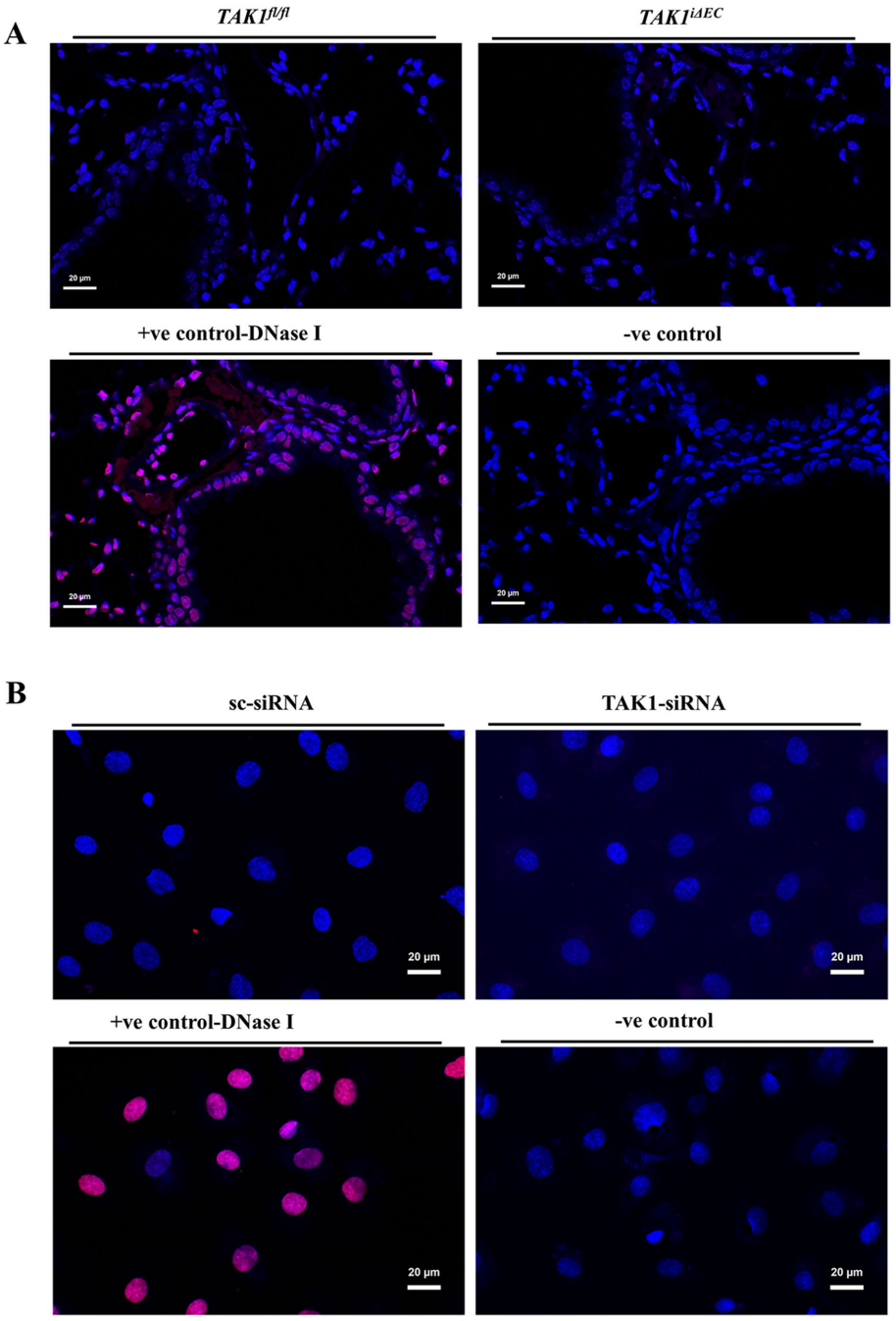

FIGURE 3: TAK1 deficiency fails to trigger apoptosis in ECs. (A) Lung sections from *TAK1*$^{fl/fl}$ and *TAK1*$^{i\Delta EC}$ mice were used for TUNEL staining to assess apoptosis of lung cells. Images were analyzed by confocal microscopy. +ve control-DNase I, *TAK1*$^{fl/fl}$-lung section treated with DNase I was used for TUNEL staining; −ve control, *TAK1*$^{fl/fl}$-lung section not treated with DNase I was used for TUNEL staining. (B) HLMVECs transfected with sc-siRNA or TAK1-siRNA (100 nM); 72 h after transfection, cells were used for TUNEL staining. Images were analyzed by confocal microscopy. Images shown are representative of two separate experiments.

TAK1 is a nodal kinase involved in activating multiple cellular signaling cascades. Global as well as EC-restricted TAK1 deletion in mice caused embryonic lethality (Sato *et al.*, 2005; Morioka *et al.*, 2012). Further, studies have demonstrated that TAK1 function in ECs is required for embryonic vascular development, angiogenesis, and prevention of EC death induced by inflammatory mediators (Morioka *et al.*, 2012; Naito *et al.*, 2019). Here we investigated whether endothelial TAK1 is required to maintain endothelial AJ integrity and to reanneal AJs after breakdown of the endothelial barrier due to vascular injury. We first used the TAK1 kinase-specific inhibitor OZ, which is widely used to study TAK1 function, and observed that blocking TAK1 kinase activity caused spontaneous loss of the endothelial barrier in an in vitro EC culture model. We also observed that OZ treatment augmented PAR-1- or TLR4-induced increase in vascular permeability in the intact lung. Next, we observed that in vivo expression of a kinase-defective TAK1 mutant in mouse lung ECs caused increased basal lung vascular permeability. To address the in vivo signaling role of TAK1 in ECs, we generated tamoxifen-inducible EC-restricted *TAK1* knockout (*TAK1*$^{i\Delta EC}$) mice and observed augmented basal lung vascular leak in *TAK1*$^{i\Delta EC}$ mice compared with WT mice. Additionally, we observed that PAR-1 or TLR-4 activation produced uncontrolled lung vascular leak in *TAK1*$^{i\Delta EC}$ mice. Consistent with these findings, we observed increased mortality in response to LPS or CLP challenge in *TAK1*$^{i\Delta EC}$ mice compared with WT mice. These results support the fundamental role of endothelial TAK1 in regulating endothelial barrier integrity.

Since previous studies have shown that endothelial TAK1 prevents vascular destruction due to TNF–α-induced EC death via apoptosis (Naito *et al.*, 2019), we measured apoptosis in WT and *TAK1*$^{i\Delta EC}$ mice. Surprisingly, we did not observe apoptotic cell death either in WT or in *TAK1*$^{i\Delta EC}$ mice under baseline conditions. Also, we did not observe EC death via apoptosis when we knocked down TAK1 in human lung ECs. These results suggest that the basal lung vascular leak observed with genetic deletion or pharmacological inhibition *of* TAK1 is likely due to destabilization of endothelial AJs but not due to apoptosis of ECs.

VE-cad and β-cat interaction at endothelial AJs stabilizes endothelial barrier integrity (Dejana *et al.*, 2008; Komarova and Malik, 2010; Carmeliet *et al.*, 1999). VE-cad directly binds to β-cat via its cytosolic domain. The VE-cad/β-cat complex is linked to the actin cytoskeleton through α-cat. Previous studies have shown that conditional inactivation of the β-cat gene in ECs causes a defective vascular pattern and increased vascular fragility (Cattelino *et al.*, 2003). Another study reported that the transcription factor FoxM1 mediates β-cat expression in ECs, which in turn is required for reannealing of the lung endothelial barrier after endothelial injury (Mirza *et al.* (2010). In addition, a recent study showed that tamoxifen-inducible EC-restricted disruption of the β-cat gene in adult mice caused blood–brain barrier breakdown (Tran *et al.*, 2016). Thus to address the molecular basis of endothelial

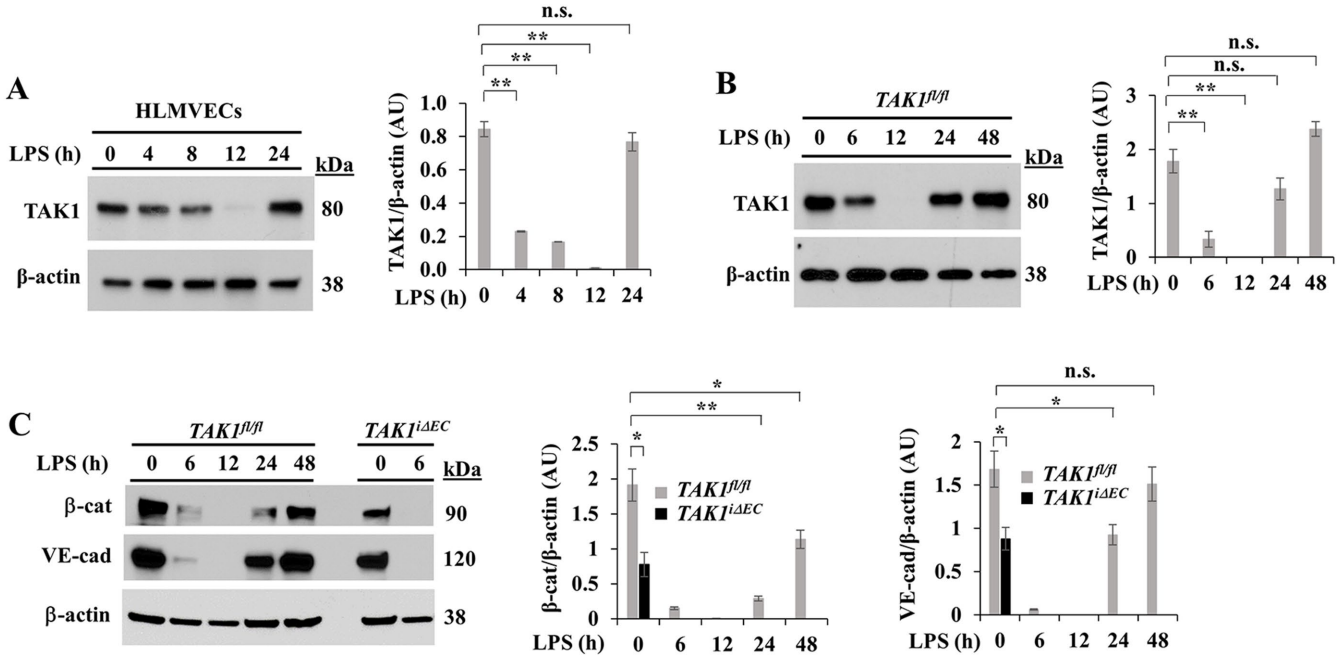

FIGURE 4: TLR4 signaling regulates endothelial AJs through TAK1 expression. (A) HLMVECs grown to confluence were treated with LPS (1 μg/ml) for different time intervals and used for IB analysis to determine TAK1 expression. Values from three experiments were expressed as mean ± SEM; n.s., not significant; $^{**}p < 0.001$ compared with 0 h LPS. (B) TAK1$^{fl/fl}$ (WT) mice were challenged with LPS (10 mg/kg, i.p.) for different time intervals. After LPS challenge, lungs were harvested for IB analysis to determine expression of TAK1. A representative IB shows expression of TAK1 in lungs of TAK1$^{fl/fl}$ mice. (C) *TAK1*$^{fl/fl}$ and *TAK1*$^{i\Delta EC}$ mice were challenged with LPS (10 mg/kg, i.p.) for different time intervals. After LPS challenge, lungs were harvested for IB analysis to determine expression of β-cat and VE-cad. A representative IB shows expression of β-cat and VE-cad in lungs of TAK1$^{fl/fl}$ and *TAK1*$^{i\Delta EC}$ mice. B-C, Values from three experiments were expressed as mean ± SEM ($N = 3$ mice per group). n.s., not significant; $^{*}p < 0.01$; $^{**}p < 0.001$.

barrier breakdown in *TAK1*$^{i\Delta EC}$ mice, we measured β-cat expression in WT and TAK1-deficient ECs. Interestingly, we found markedly reduced expression of β-cat in TAK1-deficient ECs compared with WT. We also found a similar reduction in expression of β-cat in lungs of *TAK1*$^{i\Delta EC}$ mice compared with *TAK1*$^{fl/fl}$ mice. Furthermore, we observed down-regulation of β-cat expression in ECs treated with a TAK1 inhibitor. These results suggest the possibility that TAK1 controls AJ integrity by modulating β-cat expression in ECs.

Since GSK3β regulates β-cat expression, we investigated the possible role of TAK1 in regulating GSK3β function in ECs. GSK3β is constitutively active and is inactivated by phosphorylation at S9 (Aberle *et al.*, 1997; Wang *et al.*, 2014). GSK3β-mediated phosphorylation of β-cat promotes β-cat ubiquitylation and degradation via the proteasomal pathway (Aberle *et al.*, 1997; Wang *et al.*, 2014) and thereby induces endothelial barrier breakdown. We observed that either inhibition or knockdown of TAK1 prevented baseline as well as thrombin- or LPS-induced phosphorylation of GSK3β at S9. Consistent with this observation, TAK1 inhibition increased thrombin- or LPS-induced phosphorylation and ubiquitylation of β-cat in ECs. In support of these results, we observed that inhibition of GSK3β markedly suppresses thrombin- or LPS-induced down-regulation of β-cat and permeability increase. These results collectively support the concept that TAK1-mediated inhibition of GSK3β prevents down-regulation of β-cat and hence promotes β-cat localization at AJs to maintain endothelial barrier integrity.

Next, we investigated the link between TAK1 and GSK3β in ECs and showed that TAK1 interacts with and activates AKT in ECs to phosphorylate S9 on GSK3β, thereby inhibiting GSK3β activity. We also showed that much like TAK1 inhibition, AKT inhibition induced loss of endothelial barrier function and augmented thrombin- or LPS-induced responses. We used a pharmacological approach to examine whether TAK1 is required for AKT activation. We showed that TAK1 inhibition blocked both thrombin and LPS- induced activation of AKT in ECs. In addition, AKT inhibition blocked thrombin as well as LPS-induced inactivation of GSK3β in ECs. Furthermore, AKT inhibition augmented the thrombin- or LPS-induced endothelial permeability response. These findings are in close agreement with a previous report indicating increased vascular permeability in AKT1-null mice (Chen *et al.*, 2005). Collectively, our results demonstrate that TAK1 regulates the endothelial barrier through AKT-dependent inhibition of GSK3β in ECs.

Studies have demonstrated that TAK1 is required to prevent cell death in macrophages, cancer cells, and ECs (Malireddi *et al.*, 2018; Naito *et al.*, 2019; Podder *et al.*, 2019). In our studies, under basal conditions, we did not observe EC death either in TAK1 knockdown ECs or in TAK1-null ECs. We cannot rule out the possibility that during sepsis, TAK1-null ECs undergo apoptosis to cause vascular barrier disruption. Importantly, chemical inhibition of TAK1 caused spontaneous loss of endothelial barrier function, indicating that the constitutive activity of TAK1 could regulate endothelial barrier integrity by suppressing the function of GSK3β through AKT activation. Consistent with this notion, we observed that, in *TAK1*$^{i\Delta EC}$ mice, the sepsis-induced lung vascular injury response was not reversible, indicating that TAK1-mediated AKT activation during inflammation is critical for repair of the endothelial barrier after vascular injury. In conclusion, we have identified TAK1 as an upstream signaling molecule in ECs that controls the function of GSK3β to maintain and repair the endothelial barrier after vascular injury. We believe that this novel pathway controls the restoration rate of endothelial junctions under normal physiological conditions and in the setting of

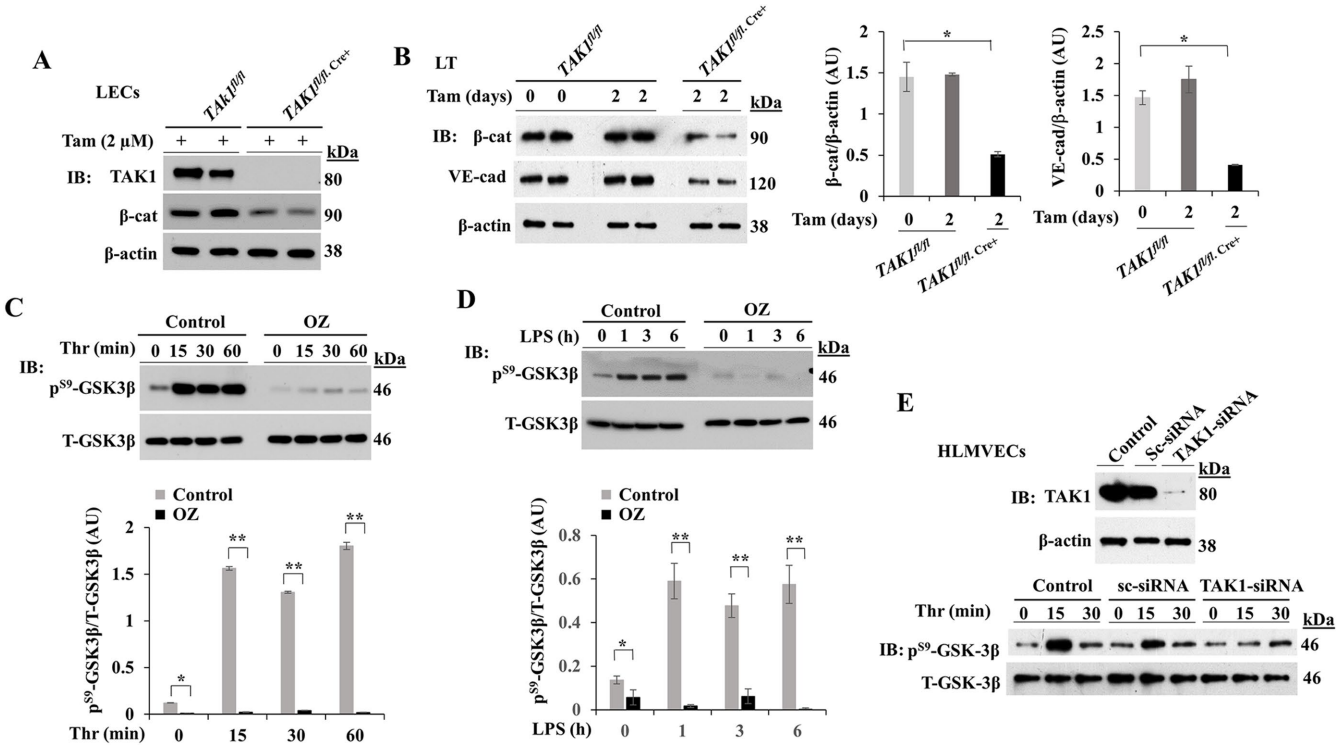

FIGURE 5: TAK1 stabilizes β-cat at endothelial AJs by inhibiting GSK3β. (A) LECs from TAK1$^{fl/fl}$ and TAK1$^{fl/fl}$. Cre+ mice were treated with tamoxifen (Tam) for 72 h and then used for IB analysis. Results shown are representative of three separate experiments. (B) TAK1$^{fl/fl}$ and TAK1$^{fl/fl}$. Cre+ mice received tamoxifen injections (1 mg/mouse/day i.p.) for 2 d and on day 7, lungs were harvested for IB analysis. Blots shown are representative of lung extracts from 6 mice per genotype. *$p < 0.01$ compared with with TAK1$^{fl/fl}$ mice. C and D, HLMVECs were treated with OZ (1 μM) or vehicle for 1 h and then exposed to either thrombin (25 nM) or LPS (1 μg/ml). Cell lysates were subjected to IB analysis to determine GSK3β phosphorylation on S-9. *$p < 0.05$; **$p < 0.001$ compared with with vehicle control. (E) HLMVECs transfected with either control-siRNA (Sc-siRNA) or TAK1-siRNA (100 nM) were used for determination of thrombin-induced phosphorylation of GSK3β on S-9. Top panel shows that TAK1 expression was suppressed in TAK1-siRNA treated cells. Bottom panel shows that TAK1 knockdown suppresses thrombin-induced S-9 phosphorylation of GSK3β. Results shown are representative of two experiments.

vascular leak. Thus targeting the TAK1-AKT-GSK3β axis represents a potential therapeutic approach to treatment of uncontrolled lung vascular leak seen in sepsis.

MATERIALS AND METHODS

Antibodies

Monoclonal antibody (mAb) against TAK1 (Cat# 4505S), polyclonal antibody (pAb) against phospho-TAK1 (Thr184/187) (Cat# 4531), pAb against p-β-cat$^{S33/37/T41}$ (Cat# 9561S), pAb against ubiquitin (Cat# 3933S), pAb against p-GSK3β^{S9} (Cat# 9322S), mAb against GSK3β (Cat# 9315S), mAb against p-AKT^{S473} (Cat# 4058S), and mAb against AKT (Cat# 4691P) were from Cell Signaling Technology (Danvers, MA). pAb against VE-cad (Cat# ab 33168) was from Abcam (Cambridge, MA). pAb against HA epitope tag (Cat# 51064-2AP) was obtained from Proteintech. pAb against β-cat (Cat# sc-7199) and pAb against CaMKKβ were obtained from Santa Cruz Biotechnology (Santa Cruz, CA). mAb against β-actin (Cat# A5441) was from Sigma (St. Loius, MO).

Other reagents

PAR-1-activating peptide (TFLLRNPNDK-NH_2) was custom synthesized as the C-terminal amide with a purity of >95% by Genscript (Piscataway, NJ). Scrambled-siRNA (Sc-siRNA) and human (*h*)-specific siRNA to target TAK1, sequences 5′-GUGCUGACAUGUCUGAAAUTT-3′; 5′-AUUUCAGACAUGUCAGCAC-3′, were custom synthesized by IDT (Coralville, IA). LPS *Escherichia coli* 0111:B4 (Cat# L3012), TAK1 inhibitor OZ (Cat# 09890), MG-132 (Cat# 474790), GSK3β inhibitor SB216763 (Cat# S3442), and AKT inhibitor (Cat# A6730) were from Sigma (St. Louis, MO). CaMKKβ inhibitor 7-Oxo-7H-benzimidazo [2,1-a]benz[de]isoquinoline-3-carboxylic acid acetate (STO-609 acetate; Cat# 1551) was from Tocris Bioscience. TAK1 expression constructs (HA-WT-TAK1 and HA-TAK1^{K63W} kinase-defective mutant) were a gift from J. Ninomiya-Tsuji (North Carolina State University, Raleigh, NC). In situ cell death detection (TUNEL Assay) kit, TMR red (Cat# 12156792910) was obtained from Roche Diagnostic.

Mice

The generation of *MAP3K7$^{flox/flox}$ (TAK1$^{fl/fl}$)* mice was described previously (Xie *et al.*, 2006). Mice were maintained in pathogen-free environment at the University of Illinois Animal Care Facility in accordance with institutional guidelines of the National Institutes of Health (NIH). All animal experiments were performed under the protocol approved by the Institutional Animal Care and Use Committee of the University of Illinois at Chicago.

Liposome-mediated gene delivery into mouse lung ECs

Liposomes were prepared as previously described by us (Zhou *et al.*, 1998; Tiruppathi *et al.*, 2014; Soni *et al.*, 2018). Briefly, the mixture comprised of dimethyldioctadecylammonium bromide and cholesterol (1:1 M ratio) was dried using the Rotavaporator

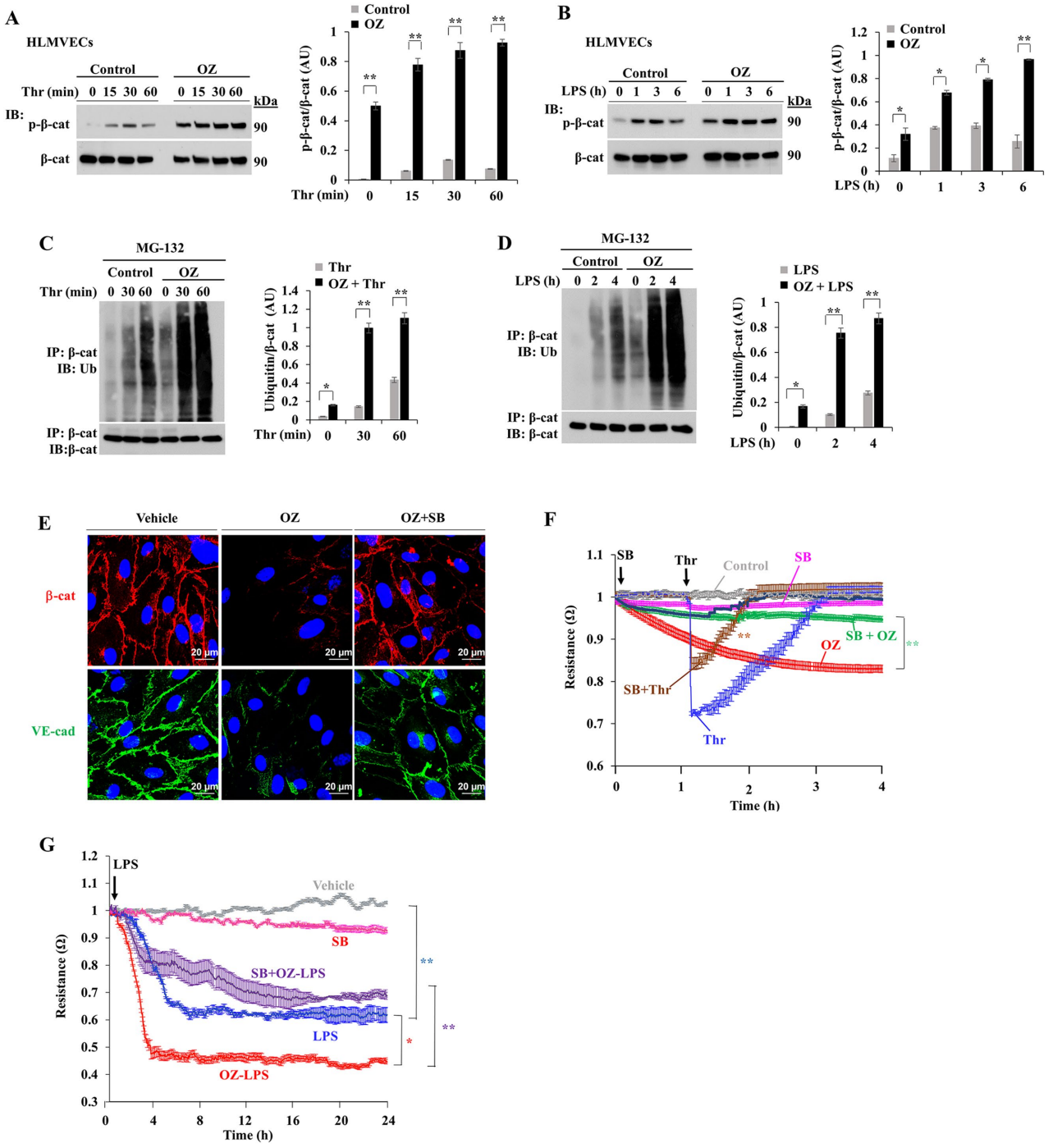

FIGURE 6: TAK1 inhibition induces β-cat degradation via a proteasomal pathway to destabilize endothelial barrier. (A, B) HLMVECs were first treated with OZ (1 μM) or vehicle for 1 h and then thrombin- or LPS-induced phosphorylation of β-cat on S33, S37, and T41 was measured. Results shown are representative of three separate experiments. Quantified data are expressed as the ratio (mean ± SEM) of phosphorylated:total protein after OZ treatment vs. control. *$p < 0.01$; **$p < 0.001$. (C, D) HLMVECs incubated with proteasomal inhibitor MG132 (10 μM) for 2 h followed by 1 μM OZ for 1 h were exposed to either thrombin (25 nM) (C) or LPS (1 μg/ml) (D) for indicated time periods. Then, cell lysates were immunoprecipitated with anti-β-cat Ab and blotted with antipan ubiquitin Ab. Quantified data from three experiments are expressed as ratio (mean ± SEM) of ubiquitin:β-cat in OZ-treated group vs. control. **$p < 0.001$. (E) HLMVECs were treated with vehicle, OZ (1 μM), or OZ (1 μM) plus SB216763 (1 μM) for 1 h followed by specific staining for β-cat (red), VE-cad (green), or nucleus (DAPI, blue). Then, cells were analyzed by confocal microscopy. (F, G) HLMVECs grown to confluence and treated with vehicle (control), 1 μM OZ, or 1 μM OZ plus 1 μM SB (SB216763) were used to measure real-time changes in TER to assess endothelial barrier integrity in response to thrombin (F) or LPS (G). Arrows indicate the time of addition of inhibitors, thrombin (25 nM), or LPS (1 μg/ml). In (F) **$p < 0.001$, OZ vs. SB + OZ, or thrombin alone vs. SB + thrombin; In G, *$p < 0.01$, LPS vs. OZ + LPS; **$p < 0.001$, vehicle vs. LPS; **$p < 0.001$, OZ+LPS vs. SB+OZ+LPS.

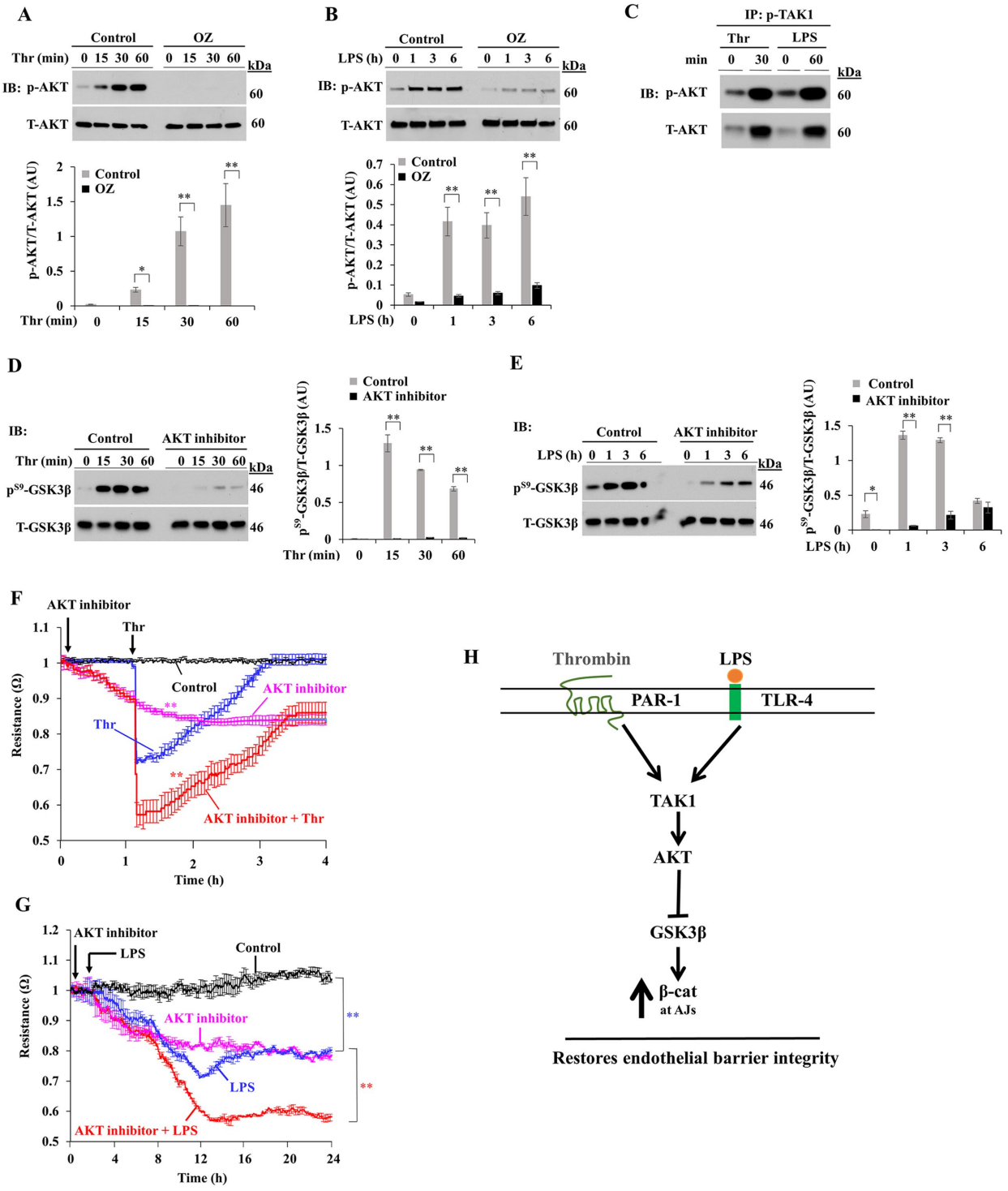

FIGURE 7: TAK1 inhibits GSK3β through AKT activation. A–C, HLMVECs treated with either vehicle (control) or 1 μM OZ for 1 h and then challenged with thrombin (A) or LPS (B) were used for IB analysis. $^{**}p < 0.001$ compared with controls. C, HLMVECs treated with thrombin or LPS were immunoprecipitated with anti-phospho-TAK1 Ab and blotted with anti-phospho-AKT Ab or anti-AKT Ab. Results shown are representative of 3 separate experiments. (D, E) HLMVECs treated either with vehicle (control) or with 1 μM AKT inhibitor for 1 h and then challenged with thrombin (D) or LPS (E) were used for IB analysis to determine S-9 phosphorylation of GSK3β. Results shown are representative of three separate experiments. $^{**}p < 0.001$ compared with controls. (F, G) HLMVECs were treated with vehicle (control) or 1 μM AKT inhibitor and then challenged with thrombin or LPS to induce real-time changes in TER for the purpose of assessing endothelial barrier integrity. Arrows indicate the time at which inhibitors, thrombin (25 nM), or LPS (1 μg/ml) were added. $^{**}p < 0.001$, AKT inhibitor vs. control, thrombin vs. AKT inhibitor plus thrombin, or LPS vs. AKT inhibitor plus LPS. H, Model of EC TAK1-dependent mechanisms of endothelial barrier repair after vascular injury. In ECs, TAK1 signaling downstream of PAR-1 or TLR4 triggers AKT activation. The activated AKT phosphorylates GSK3β on S9 to inactivate GSK3β, which in turn prevents β-cat degradation via the proteasomal pathway and thereby stabilizes AJs.

(Brinkmann) and dissolved in 5% glucose followed by 20 min sonication. The complex consisting of plasmid DNA expressing HA-WT-TAK1 or kinase-defective mutant TAK1 (HA-TAK1^{K63W}) and liposomes were combined at a ratio of 1 µg of DNA to 8 nmol of liposomes. The DNA/liposome complex (30 µg of DNA/mouse) 100 µl was injected into the retro-orbital venous plexus (Zhou *et al*, 1998; Tiruppathi *et al.*, 2014; Soni *et al.*, 2018). Seventy-two hours after injection, mice were used for experiments.

Generation of inducible EC-restricted *TAK1* knockout (*TAK1*$^{i\Delta EC}$) Mice

TAK1$^{fl/fl}$ mice were bred with *End-SCL-Cre-ER(T)* mice containing tamoxifen-inducible Cre-ER(T) driven by 5′ endothelial enhancer of the stem cell leukemia locus (Mittal *et al.*, 2017; Göthert *et al.*, 2004) to generate *TAK1*$^{fl/fl\text{-}Cre\text{-}}$ (WT) and TAK1$^{fl/fl\text{-}Cre+}$ mice. *TAK1*$^{fl/fl\text{-}Cre\text{-}}$ and TAK1$^{fl/fl\text{-}Cre+}$ mice were administered tamoxifen (1 mg/mouse) i.p for 2 consecutive days to generate EC-restricted inducible TAK1 knockout (*TAK1*$^{i\Delta EC}$) mice.

Lung injury in mice

Experimental lung injury was induced by systemic LPS (i.p.) in mice (Tiruppathi *et al.*, 2014). Lung injury was assessed by pulmonary capillary filtration coefficient ($K_{f,c}$) measurement using isolated lung preparations (Tiruppathi *et al.*, 2002) and in vivo EBA uptake in lungs (Soni *et al.*, 2017, 2018). For histology, paraffin-embedded sections 5 µm in thickness prepared from the lungs were stained with hematoxylin and eosin. Polymicrobial sepsis was induced by CLP method as described (Rittirsch *et al.*, 2008). Caecum was punctured using an 18-gauge needle on five different places. For survival studies, mice were monitored four times daily.

Cells, siRNA transfection, and apoptosis

HLMVECs were cultured in EGM-2MV supplemented with 15% fetal bovine serum (FBS) as described (Soni *et al.*, 2017). Mouse (C57BL/6) lung ECs were isolated and cultured as described previously (Tiruppathi *et al.*, 2002). Both cell types were used between passages 3 and 6. HLMVECs grown to 70–80% confluence on gelatin-coated culture dishes were transfected with target siRNAs or sc-siRNA as described (Soni *et al.*, 2017). At 72 h after transfection, cells were used for experiments. Bone marrow-derived macrophages (BMDMs) from mice were generated by culture of bone marrow cells as described (Mittal *et al.*, 2016). EC apoptosis was determined by TUNEL staining using an in situ cell death detection kit, TMR red from Roche Diagnostic.

Transendothelial electrical resistance measurement

Real-time changes in transendothelial monolayer electrical resistance (TER) were measured to assess endothelial barrier function (Tiruppathi *et al.*, 1992). A confluent endothelial monolayer incubated with 2% FBS containing medium was exposed to indicated inhibitors, thrombin, or LPS. Data are presented as resistance normalized to its starting value zero time.

Immunostaining

ECs grown on glass coverslips were washed with HBSS and fixed with 2% paraformaldehyde for 20 min. Cells were permeabilized with 0.1% Triton X-100 for 15 min at 4°C. Next, cells were blocked in 5% goat serum in HBSS for 1 h at room temperature, incubated with primary antibody overnight at 4°C, followed by incubation with Alexa-Fluor–conjugated secondary antibody and 4′,6-diamidino-2-phenylindole (DAPI) for 1 h at room temperature. In each step, cells were washed three times with HBSS. Coverslips were mounted with prolong gold antifade reagent (Invitrogen) on glass slides. Images were acquired with the Zeiss LSM 510 confocal microscope.

Immunoprecipitation and immunoblotting

ECs grown to confluence treated with or without specific agents were washed three times with phosphate-buffered saline at 4°C and lysed in lysis buffer (50 mM Tris-HCl, pH 7.5, 150 mM NaCl, 1 mM EGTA, 1% Triton X-100, 0.25% sodium deoxycholate, 0.1% SDS, 10 µM orthovanadate, and protease-inhibitor mixture as described Soni *et al.* [2017]). Mouse lungs were homogenized in lysis buffer (Soni *et al.*, 2017). EC lysates or mouse lung homogenates were centrifuged (13,000 × *g* for 10 min) to remove insoluble materials. The clear supernatant collected was subjected to immunoblot (IB) analysis or immunoprecipitation. Each sample was incubated overnight with 1 µg/ml the indicated antibody at 4°C. The next day, Protein A/G beads were added to the sample and incubated at 4°C for 1 h. Immunoprecipitates were then washed three times with wash buffer (Tris-buffered saline containing 0.05% Triton X-100, 1 mM Na_3VO_4, 1 mM NaF, 2 µg/ml leupeptin, 2 µg/ml pepstatin A, 2 µg/ml aprotinin, and 44 µg/ml phenylmethylsulfonyl fluoride) and used for IB analysis. EC lysates, lung tissue extracts, or immunoprecipitated proteins were resolved by SDS–PAGE on a 4–15% gradient or 6% separating gel under reducing conditions and transferred to a polyvinylidene difluoride membrane. Membranes were blocked with 5% dry milk in TBST (10 mM Tris-HCl, pH7.5, 150 nM NaCl, and 0.05% Tween-20) at RT for 1 h. Membranes were then probed with the indicated primary antibody (diluted in blocking buffer) overnight at 4°C. Next, membranes were washed three times and then incubated with appropriate HRP–conjugated secondary antibody. Protein bands were detected by enhanced chemiluminescence. IB bands were quantified using NIH ImageJ software.

Statistical analysis

ANOVA, Student's *t* test (two-tailed), and log-rank test were used to determine statistical significance with a *P* value threshold set at <0.05.

ACKNOWLEDGMENTS

This work was supported by National Institutes of Health Grants R01 GM-117028, R01HL156965, and R01GM138499.

REFERENCES

Aberle H, Bauer A, Stappert J, Kispert A, Kemler R (1997). Beta-catenin is a target for the ubiquitin-proteasome pathway. EMBO J 16, 3797–3804.

Adhikari A, Xu M, Chen ZJ (2007). Ubiquitin-mediated activation of TAK1 and IKK. Oncogene 26, 3214–3226.

Ajibade AA, Wang Q, Cui J, Zou J, Xia X, Wang M, Tong Y, Hui W, Liu D, Su B, *et al.* (2012). TAK1 negatively regulates NF-κB and p38 MAP kinase activation in Gr-1+CD11b+ neutrophils. Immunity 36, 43–54.

Carmeliet P, Lampugnani MG, Moons L, Breviario F, Compernolle V, Bono F, Balconi G, Spagnuolo R, Oosthuyse B, Dewerchin M, *et al.* (1999). Targeted deficiency or cytosolic truncation of the VE-cadherin gene in mice impairs VEGF-mediated endothelial survival and angiogenesis. Cell 98, 147–157.

Cattelino A, Liebner S, Gallini R, Zanetti A, Balconi G, Corsi A, Bianco P, Wolburg H, Moore R, Oreda B, *et al.* (2003). The conditional inactivation of the beta-catenin gene in endothelial cells causes a defective vascular pattern and increased vascular fragility. J Cell Biol 162, 1111–1122.

Chen J, Somanath PR, Razorenova O, Chen WS, Hay N, Bornstein P, Byzova TV (2005). Akt1 regulates pathological angiogenesis, vascular maturation and permeability in vivo. Nat Med 11, 1188–1196.

Chen XL, Nam JO, Jean C, Lawson C, Walsh CT, Goka E, Lim ST, Tomar A, Tancioni I, Uryu S, *et al.* (2012). VEGF-induced vascular permeability is mediated by FAK. Dev Cell 22, 146–157.

Cohen P, Frame S (2001). The renaissance of GSK3. Nat Rev Mol Cell Biol 2, 769–776.

Dejana E, Orsenigo F, Lampugnani MG (2008). The role of adherens junctions and VE-cadherin in the control of vascular permeability. J Cell Sci 121, 2115–2122.
Fechtner S, Fox DA, Ahmed S (2017). Transforming growth factor β activated kinase 1: a potential therapeutic target for rheumatic diseases. Rheumatology (Oxford) 56, 1060–1068.
Goddard LM, Iruela-Arispe ML (2013). Cellular and molecular regulation of vascular permeability. Thromb Haemost 109, 407–415.
Goldenberg NM, Steinberg BE, Slutsky AS, Lee WL (2011). Broken barriers: a new take on sepsis pathogenesis. Sci Transl Med 3, 88ps25.
Gong H, Gao X, Feng S, Siddiqui MR, Garcia A, Bonini MG, Komarova Y, Yogel SM, Mehta D, Malik AB (2014). Evidence of a common mechanism of disassembly of adherens junctions through Galpha13 targeting of VE-cadherin. J Exp Med 211, 579–591.
Göthert JR, Gustin SE, van Eekelen JA, Schmidt U, Hall MA, Jane SM, Green AR, Göttgens B, Izon DJ, Begley CG (2004). Genetically tagging endothelial cells in vivo: bone marrow-derived cells do not contribute to tumor endothelium. Blood 104, 1769–1777.
Ishitani T, Kishida S, Hyodo-Miura J, Ueno N, Yasuda J, Waterman M, Shibuya H, Moon RT, Ninomiya-Tsuji J, Matsumoto K (2003). The TAK1-NLK mitogen-activated protein kinase cascade functions in the Wnt-5a/Ca^{2+} pathway to antagonize Wnt/β-catenin signaling. Mol Cell Biol 23,131–139.
Komarova Y, Malik AB (2010). Regulation of endothelial permeability via paracellular and transcellular transport pathways. Annu Rev Physiol 72, 463–493.
Liu HH, Xie M, Schneider MD, Chen ZJ (2006). Essential role of TAK1 in thymocyte development and activation. Proc Natl Acad Sci USA 103, 11677–11682.
Malireddi RKS, Gurung P, Mavuluri J, Dasari TK, Klco JM, Chi H, Kanneganti TD (2018). TAK1 restricts spontaneous NLRP3 activation and cell death to control myeloid proliferation. J Exp Med 215, 1023–1034.
Matthay MA, Zemans RL (2011). The acute respiratory distress syndrome pathogenesis and treatment. Annu Rev Pathol 6, 147–163.
Matthay MA, Zemans RL, Zimmerman GA, Arabi YM, Beitler JR, Mercat A, Herridge M, Randolph AG, Calfee CS (2019). Acute respiratory distress syndrome. Nat Rev Dis Primers 5, 18.
Mirza MK, Sun Y, Zhao YD, Potula HH, Frey RS, Vogel SM, Malik AB, Zhao YY (2010). FoxM1 regulates re-annealing of endothelial adherens junctions through transcriptional control of beta-catenin expression. J Exp Med 207, 1675–1685.
Mittal M, Nepal S, Tsukasaki Y, Hecquet CM, Soni D, Rehman J, Tiruppathi C, Malik AB (2017). Neutrophil activation of endothelial cell-expressed TRPM2 mediates transendothelial neutrophil migration and vascular injury. Circ Res 121, 1081–1091.
Mittal M, Tiruppathi C, Nepal S, Zhao YY, Grzych D, Soni D, Prockop DJ, Malik AB (2016). TNF-α-stimulated gene-6 (TSG6) activates macrophage phenotype transition to prevent inflammatory lung injury. Proc Natl Acad Sci USA 113, E8151–E8158.
Morioka S, Inagaki M, Komatsu Y, Mishina Y, Matsumoto K, Ninomiya-Tsuji J (2012). TAK1 kinase signaling regulates embryonic angiogenesis by modulating endothelial cell survival and migration. Blood 120, 3846–3857.
Naito H, Iba T, Wakabayashi T, Tai-Nagara I, Suehiro JI, Jia W, Eino D, Sakimoto S, Muramatsu F, Kidoya H, *et al*. (2019). TAK1 prevents endothelial apoptosis and maintains vascular integrity. Dev Cell 48,151–166.
Ninomiya-Tsuji J, Kishimoto K, Hiyama A, Inoue J, Cao Z, Matsumoto K (1999). The kinase TAK1 can activate the NIK-I kappaB as well as the MAP kinase cascade in the IL-1 signalling pathway. Nature 398, 252–256.
Nottebaum AF, Cagna G, Winderlich M, Gamp AC, Linnepe R, Polaschegg C, Filippova K, Lyck R, Engelhardt B, Kamenyeva O, *et al*. (2008). VE-PTP maintains the endothelial barrier via plakoglobin and becomes dissociated from VE-cadherin by leukocytes and by VEGF. J Exp Med 205, 2929–2945.
Orsenigo F, Giampietro C, Ferrari A, Corada M, Galaup A, Sigismund S, Ristagno G, Maddaluno L, Koh GY, Franco D, *et al*. (2012). Phosphorylation of VE-cadherin is modulated by haemodynamic forces and contributes to the regulation of vascular permeability in vivo. Nat Commun 3, 1208.
Podder B, Guttà C, Rožanc J, Gerlach E, Feoktistova M, Panayotova-Dimitrova D, Alexopoulos LG, Leverkus M, Rehm M (2019). TAK1 suppresses RIPK1-dependent cell death and is associated with disease progression in melanoma. Cell Death Differ. DOI 10:1038/s41418-019-0315-8.
Ramirez SH, Fan S, Dykstra H, Rom S, Mercer A, Reichenbach NL, Gofman L, Persidsky Y (2013). Inhibition of glycogen synthase kinase 3β promotes tight junction stability in brain endothelial cells by half-life extension of occludin and claudin-5. PLoS One 8, e55972.
Ridder DA, Lang MF, Salinin S, Röderer JP, Struss M, Maser-Gluth C, Schwaninger M (2011). TAK1 in brain endothelial cells mediates fever and lethargy. J Exp Med 208, 2615–2623.
Rittirsch D, Huber-Lang MS, Flierl MA, Ward PA (2008). Immunodesign of experimental sepsis by cecal ligation and puncture. Nat Protoc 4, 31–36.
Sato S, Sanjo H, Takeda K, Ninomiya-Tsuji J, Yamamoto M, Kawai T, Matsumoto K, Takeuchi O, Akira S (2005). Essential function for the kinase TAK1 in innate and adaptive immune responses. Nat Immunol 6, 1087–1095.
Schuman J, Chen Y, Podd A, Yu M, Liu HH, Wen R, Chen ZJ, Wang D (2009). A critical role of TAK1 in B-cell receptor-mediated nuclear factor kappaB activation. Blood 113, 4566–4574.
Shim JH, Xiao C, Paschal AE, Bailey ST, Rao P, Hayden MS, Lee KY, Bussey C, Steckel M, Tanaka N, *et al*. (2007). TAK1, but not TAB1 or TAB2, plays an essential role in multiple signaling pathways in vivo. Genes Dev 19, 2668–2681.
Singhirunnusorn P, Suzuki S, Kawasaki N, Saiki I, Sakurai H (2005). Critical roles of threonine 187 phosphorylation in cellular stress-induced rapid and transient activation of transforming growth factor-beta-activated kinase 1 (TAK1) in a signaling complex containing TAK1-binding protein TAB1 and TAB2. J Biol Chem 280, 7359–7368.
Soni D, Regmi SC, Wang DM, DebRoy A, Zhao YY, Vogel SM, Malik AB, Tiruppathi C (2017). Pyk2 phosphorylation of VE-PTP downstream of STIM1-induced Ca^{2+} entry regulates disassembly of adherens junctions. Am J Physiol Lung Cell Mol Physiol 312, L1003–L1017.
Soni D, Wang DM, Regmi SC, Mittal M, Vogel SM, Schlüter D, Tiruppathi C (2018). Deubiquitinase function of A20 maintains and repairs endothelial barrier after lung vascular injury. Cell Death Discov 4, 60.
Sundivakkam PC, Natarajan V, Malik AB, Tiruppathi C (2013). Store-operated Ca^{2+} entry (SOCE) induced by protease-activated receptor-1 mediates STIM1 protein phosphorylation to inhibit SOCE in endothelial cells through AMP-activated protein kinase and p38β mitogen-activated protein kinase. J Biol Chem 288, 17030–17041.
Tiruppathi C, Freichel M, Vogel SM, Paria BC, Mehta D, Flockerzi V, Malik AB (2002). Impairment of store-operated Ca^{2+} entry in $TRPC4^{-/-}$ mice interferes with increase in lung microvascular permeability. Circ Res 91, 70–76.
Tiruppathi C, Malik AB, Del Vecchio PJ, Keese CR, Giaever I (1992). Electrical method for detection of endothelial cell shape change in real time: assessment of endothelial barrier function. Proc Natl Acad Sci USA 89, 7919–7923.
Tiruppathi C, Soni D, Wang DM, Xue J, Singh V, Thippegowda PB, Cheppudira BP, Mishra RK, Debroy A, Qian Z, *et al*. (2014). The transcription factor DREAM represses the deubiquitinase A20 and mediates inflammation. Nat Immunol 15, 239–247.
Tran KA, Zhang X, Predescu D, Huang X, Machado RF, Göthert JR, Malik AB, Valyi-Nagy T, Zhao YY (2016). Endothelial β-catenin signaling is required for maintaining adult blood-brain barrier integrity and central nervous system homeostasis. Circulation 133:177–186.
Wang C, Deng L, Hong M, Akkaraju GR, Inoue J, Chen ZJ (2001). TAK1 is ubiquitin-dependent kinase of MKK and IKK. Nature 412, 346–351.
Wang H, Kumar A, Lamont RJ, Scott DA (2014). GSK3β and the control of infectious bacterial diseases. Trends Microbiol 22, 208–217.
Wessel F, Winderlich M, Holm M, Frye M, Rivera-Galdos R, Vockel M, Linnepe R, Ipe U, Stadtmann A, Zarbock A, *et al*. (2014). Leukocyte extravasation and vascular permeability are each controlled in vivo by different tyrosine residues of VE-cadherin. Nat Immunol 15, 223–230.
Xie M, Zhang D, Dyck JR, Li Y, Zhang H, Morishima M, Mann DL, Taffet GE, Baldini A, Khoury DS, *et al*. (2006). A pivotal role for endogenous TGF-beta-activated kinase-1 in the LKB1/AMP-activated protein kinase energy-sensor pathway. Proc Natl Acad Sci USA 103, 17378–17383.
Yang L, Joseph S, Sun T, Hoffmann J, Thevissen S, Offermanns S, Strilic B (2019). TAK1 regulates endothelial cell necroptosis and tumor metastasis. Cell Death Differ doi: 10.1038/s41418-018-0271-8.
Zhou MY, Lo SK, Bergenfeldt M, Tiruppathi C, Jaffe A, Xu N, Malik AB (1998). In vivo expression of neutrophil inhibitory factor via gene transfer prevents lipopolysaccharide-induced lung neutrophil infiltration and injury by a β2 integrin-dependent mechanism. J Clin Invest 101, 2427–2437.